

Neural Video Fields Editing

Shuzhou Yang^{1,2} Chong Mou¹ Jiwen Yu¹ Yuhan Wang^{1,2}
 Xiandong Meng² Jian Zhang¹✉

¹SECE, Peking University

²Peng Cheng Laboratory

<https://nvedit.github.io/>

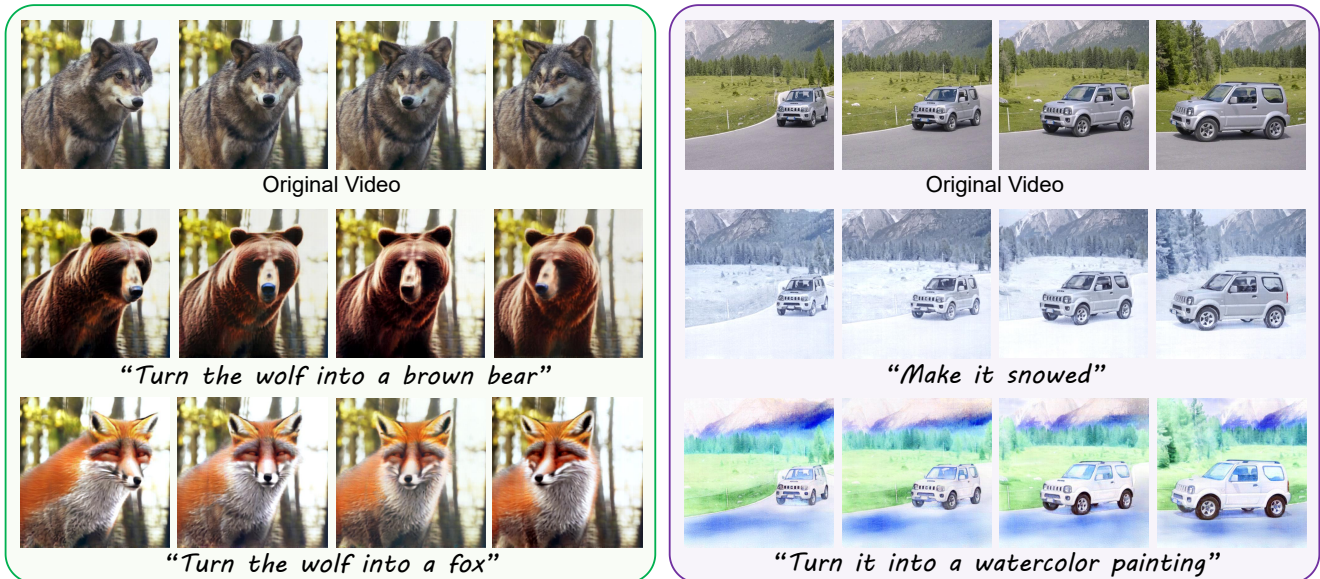


Figure 1. **NVEdit** enables various editing options, including shape variation, scene change, and style transfer, while preserving the motion and semantic layout of the original scene. Due to its efficient encoding rate, long videos with hundreds of frames even be edited well.

Abstract

Diffusion models have revolutionized text-driven video editing. However, applying these methods to real-world editing encounters two significant challenges: (1) the rapid increase in graphics memory demand as the number of frames grows, and (2) the inter-frame inconsistency in edited videos. To this end, we propose **NVEdit**, a novel text-driven video editing framework designed to mitigate memory overhead and improve consistent editing for real-world long videos. Specifically, we construct a neural video field, powered by tri-plane and sparse grid, to enable encoding long videos with hundreds of frames in a memory-efficient manner. Next, we update the video field through off-the-shelf Text-to-Image (T2I) models to impart text-driven editing effects. A progressive optimization strategy is developed to preserve original temporal priors. Importantly, both the neural video field and T2I model are adaptable and replaceable, thus inspiring future research. Experiments

demonstrate that our approach successfully edits hundreds of frames with impressive inter-frame consistency.

1. Introduction

Text-driven video editing aims to faithfully edit high-quality videos following the user-given prompts. Due to the limited paired video-prompt data, using videos to train models is expensive [33, 39]. Considering the advancement of Text-to-Image (T2I) methods [11, 22, 27], adopting the pre-trained T2I models to edit videos has attracted wide attention [5, 8, 26, 46]. However, T2I models inherently lack cross-frame semantic consistency, resulting in inevitable flickering between edited frames. Hence, editing videos more temporal-consistently has become a challenging task.

In pursuit of this objective, numerous algorithms improve cross-attention operations [47, 49] and DDIM [41] inversion [4, 25, 38] to ensure superior generation and inter-

frame coherence. However, these methods still exhibit two principal deficiencies. First, although various constraints and attention control are introduced to the generation process, inter-frame inconsistency still exhibits in the edited videos, such as object deformation and texture variation. That is because T2I models inherently lack temporal motion priors. The second drawback is the rapid increase in graphics memory demands as more frames are edited, while limited hardware devices constrain the length of videos they can edit. Since editing long videos with hundreds of frames is significant for real-world applications, existing T2I models cannot achieve satisfactory effects in videos. Neural representation [7, 19, 24] may be a feasible tool to decrease memory overhead while improving inter-frame consistency, since it has a high compression rate for videos and models contents well. Some current works have tried this proposal [15, 29] but brought other limitations, such as inaccuracies in complex motion or viewpoint changing, *etc.*

To address these challenges, a memory-efficient framework is developed for consistent text-driven video editing, avoiding intricate attention-related operations or fine-tuning for T2I models. Inspired by [10], validating the use of a T2I model for updating neural radiance fields in editing 3D scenes, we extend this concept to video signals through a Neural Video Field (NVF). Specifically, our approach comprises two stages: **video fitting** and **field editing**. In the first stage, we construct an NVF with tri-plane encoding and sparse grids, efficiently modeling temporal and content priors of a given video. Benefiting from its encoding efficiency, even lengthy videos with hundreds of frames can be represented as a signal field. In the second stage, the trained NVF is updated to incorporate text-based editing effects. During each iteration, NVF renders a frame, and a T2I model is employed to edit it based on the provided text. These edited frames serve as pseudo Ground Truths (GTs) to optimize the parameters of NVF. Since NVF has been initially trained on the original video, it retains robust temporal priors post-optimization while manifesting the desired editing effects. This strategy of using Neural Video fields for video **Editing** is termed **NVEdit**. Our NVEdit possesses inherent intriguing properties of neural representation, *e.g.*, frame interpolation, which has been explored in recent works [7, 17]. During inference, NVEdit predicts frames not present in the original video seamlessly, while exhibiting coherent editing effects. In addition, both the NVF and the T2I model within NVEdit are adaptable, allowing for seamless improvements or replacements based on diverse requirements. In this paper, we majorly adopt Instruct-Pix2Pix (IP2P) [3] for editing effects. We observed that for local editing, IP2P tends to modify regions that should be preserved inaccurately, impacting video editing outcomes. To address this, an auxiliary mask is designed to constrain the editable region without additional calcula-

tion, resulting in Instruct-Pix2Pix+ (IP2P+). This version not only enhances local editing capabilities but also demonstrates the potential for T2I model improvement within NVEdit. Overall, our contributions are as follows:

- We develop NVEdit, using a neural video field to fit long videos and refining it with off-the-shelf T2I models for editing effects. It allows for seamless improvement or replacement of both the T2I models and the video field.
- We propose an auxiliary mask to promote the local editing capability of IP2P, thus benefiting our video editing. It also highlights our potential for T2I model improvement.
- Extensive experiments demonstrate that the proposed method edits long videos with hundreds of frames more consistently while exhibiting promising editing effects.
- NVEdit capitalizes on the unique properties of neural representation, including frame interpolation. The interpolated frames exhibit coherent editing effects seamlessly, without any fine-tuning or post-processing operations.

2. Related Work

2.1. Text-driven Video Editing

Editing videos through user-given texts has attracted wide attention. A straightforward idea is to train a model with video-text pairs. Ho *et al.* [13] first proposed to train a diffusion model from videos and images but required paired video-text data, which is expensive to obtain. To reduce the reliance on video data, Singer *et al.* [39] learned visual-text correlation from paired image-text data and captured motion information from videos. Qin *et al.* [33] synthesized video-prompt triplets with off-the-shelf models, but training with video data is expensive. As the advancement of conditional diffusion models [1, 30, 35] promotes text-to-image generation [18, 28, 36, 37, 42, 52], exploiting their effective vision priors to edit videos has attracted wide attention. The key challenge is ensuring inter-frame consistency. Wu *et al.* [47] fine-tuned a T2I model to fit a specific video for temporal modeling. Khachatryan *et al.* [16] simulated motions by translating latent. Qi *et al.* [32] fused attention features before and after editing for consistency. Wang *et al.* [43] developed dense spatial-temporal attention to learn motion. Geyer *et al.* [9] only edited key frames and propagated to the whole video. Liew *et al.* [20] decoupled content, structure, and motion signals to model coherent features. However, these methods require rapid increased memory to edit more frames, limiting the potential for editing long videos.

To this end, NVEdit encodes videos in a memory-efficient manner to achieve long video editing, which has more significant value in practical application.

2.2. Neural Representation for Videos

Using coordinate-based neural networks to represent visual signals is an emerging practical technology [2, 17, 19, 45,

48]. Sitzmann *et al.* [40] first encoded a video by a network, whose input is the spatio-temporal coordinate (x, y, t) and output is a pixel value. But its reconstruction quality is limited and training takes too long. To this end, Chen *et al.* [7] replaced input with the time stamp t to output the t -th frame of the target video for better performance. Li *et al.* [19] disentangled spatio-temporal context to accelerate mapping from the input coordinates to the output frames. Bai *et al.* [2] chose to divide a frame into several patches, which reduces training difficulty and improves fitting accuracy. Kim *et al.* [17] developed an explicit-implicit hybrid structure to improve fitting speed and accuracy greatly.

Recently, some attempts at video editing appeared. Kasen *et al.* [15] utilized Multilayer Perceptrons (MLPs) to map video pixels to Atlas maps, and edited videos by editing the Atlas maps. Further, Ouyang *et al.* [29] mapped video content to a canonical image and edited it to realize video editing. However, the strategy of extracting video content to a representation medium and editing it naturally has two disadvantages. First, for videos with significant content changes (such as large movements or long range motion), it is hard to map all content to a single medium, which limits accuracy. Second, their editing effect relies entirely on the image editing of the medium. But T2I models may perform poorly in some cases, *i.e.*, lack robustness.

In this paper, we optimize a well-designed neural video field for editing. It not only maintains temporal consistency but is also robust to T2I model failures in certain situations.

3. Method

Our goal is to edit videos based on user-given instructions. In Sec. 3.1, we first introduce some preliminaries, including latent diffusion models, a well-known T2I tool (Instruct-Pix2Pix [3]), and the principles of the neural video field. Then, we discuss the details of NVEdit in Sec. 3.2. It attains temporal priors in the fitting stage and imparts editing effects with a neural video field. Finally, in Sec. 3.3, we showcase IP2P+, an enhanced version of IP2P, to improve editing quality. In this paper, we majorly adopt IP2P+ for editing effects. However, it is worth noting that both the video field and T2I model are replaceable and improvable.

3.1. Preliminaries

Latent Diffusion Models (LDMs). LDMs [35] encode the input image to a latent embedding \mathbf{z}_0 , and receive a prompt P as the condition, which is also encoded to an embedding \mathbf{c}_P . Following DDPM [12], according to the step t , \mathbf{z}_0 is diffused to \mathbf{z}_t through random noise ε . LDMs aim to predict the added noise by minimizing the following objective:

$$\min_{\theta} \mathbb{E}_{\mathbf{z}_0, \varepsilon \sim \mathcal{N}(0, I), t} \|\varepsilon - \varepsilon_{\theta}(\mathbf{z}_t, t, \mathbf{c}_P)\|_2^2. \quad (1)$$

During inference, given a random latent \mathbf{z}_T and a prompt P , the trained model predicts noise $\varepsilon_{\theta}(\cdot)$ for T steps to gener-

ate an image, which meets the textual condition P .

Instruct-Pix2Pix. Based on LDMs which incorporate textual condition \mathbf{c}_P , IP2P [3] introduces an image condition \mathbf{c}_I to generate images that exhibit similar semantic layouts to \mathbf{c}_I while adhering to \mathbf{c}_P . Given a random embedding \mathbf{z}_T , IP2P predicts noise $\varepsilon_{\theta}(\cdot)$ for T steps to get results. At each step t , its predicted noise can be expressed as:

$$\begin{aligned} \varepsilon_{\theta}(\mathbf{z}_t, \mathbf{c}_I, \mathbf{c}_P) = & \varepsilon_{\theta}(\mathbf{z}_t, \emptyset, \emptyset) \\ & + s_I \cdot (\varepsilon_{\theta}(\mathbf{z}_t, \mathbf{c}_I, \emptyset) - \varepsilon_{\theta}(\mathbf{z}_t, \emptyset, \emptyset)) \\ & + s_P \cdot (\varepsilon_{\theta}(\mathbf{z}_t, \mathbf{c}_I, \mathbf{c}_P) - \varepsilon_{\theta}(\mathbf{z}_t, \mathbf{c}_I, \emptyset)), \end{aligned} \quad (2)$$

where s_I and s_P are the weights for image and text conditions respectively. The first term means random sampling, the second term guides sampling based on the image condition, while the third term introduces the textual condition.

Neural video fields. Recent works propose to represent video information through neural networks [7, 17, 51], which can mainly be simplified to a mapping function as:

$$\tilde{\mathbf{V}}[x, y, t] = f_{\theta}(x, y, t), \quad (3)$$

where t is the temporal stamp of a frame in the video, x and y are the horizontal and vertical coordinates of a pixel on the frame. $\tilde{\mathbf{V}}$ is the target video signal. Their training purpose is to update parameters θ to fit the given video. During inference, given the coordinates of all pixels from a video, the model $f_{\theta}(\cdot)$ will output the entire video.

3.2. NVEdit

In this section, we discuss how to build a Neural Video Field (NVF) to achieve editing in a memory-efficient manner. We first introduce the structure of NVF, then showcase the process of video fitting, field editing, and inference.

Model structure. NVP [17] validates that the explicit-implicit hybrid structures benefit fitting speed and accuracy. We thus build a hybrid model to represent video signals. As shown in the left part of Fig. 2, our explicit module contains tri-plane and sparse grids. The former is three feature maps designed to record video features and the latter is a set of parameter grids sparsely distributed across the $x - y - t$ coordinate system of the video. Both of them are trainable parameters, denoted as θ_{ex} . Given a spatio-temporal coordinate (x, y, t) , we extract features from its neighbor grids and tri-plane, represented as the white cube in Fig. 2. Our implicit part is an MLP that decodes the aggregated features into a pixel value, whose parameters are θ_{im} . We update $\theta = \{\theta_{im}, \theta_{ex}\}$ to fit a video \mathbf{V} and achieve editing effects.

Video fitting stage. In each iteration, we randomly sample a batch of pixels from \mathbf{V} , denoted as $\mathbf{V}[\psi]$, and their spatio-temporal coordinates set ψ . $\mathbf{V}[\psi]$ are considered as the Ground Truths (GTs) and ψ serves as the input for NVF, based on which NVF predicts pixel values. We enforce its

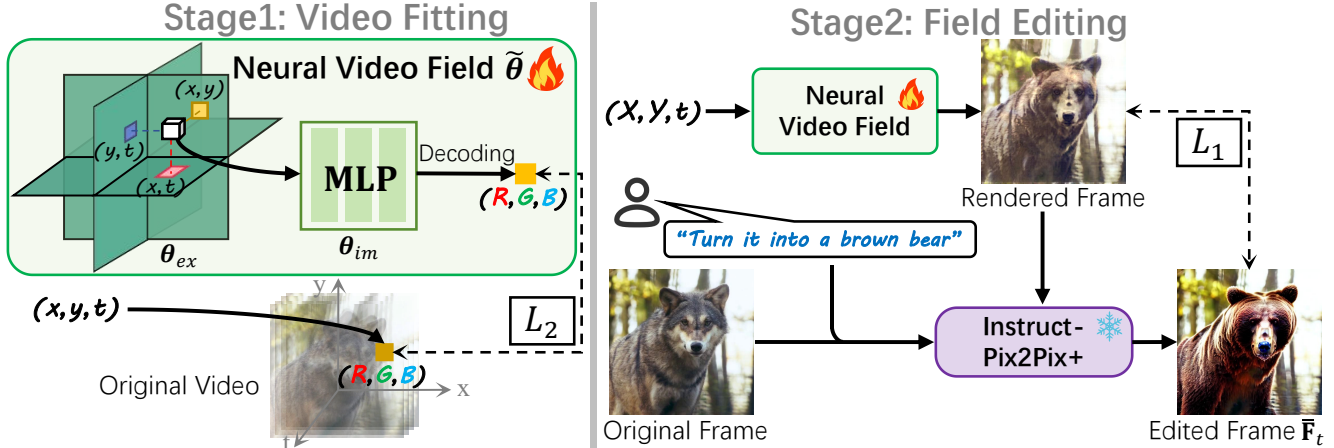


Figure 2. Workflow of our NVEdit. It contains two stages: video fitting and field editing. As shown in the left part, we first train a neural video field to fit a given video for temporal priors. Then, on the right, the rendered frame is edited and used to optimize the trained field to impart editing effects. As the video field has learned temporal priors, the optimized field consistently renders a video with edited content.

output to be similar to GT, expressed as:

$$\mathcal{L}_{\text{fit}}(\tilde{\theta}) = \sum_{(x,y,t) \in \psi} \|\mathbf{V}[x,y,t] - \tilde{f}_{\tilde{\theta}}(x,y,t)\|_2^2. \quad (4)$$

As the batch size is independent of the video length, our graphics memory demand remains constant. Notably, we supervise training with randomly sampled pixels across the entire video rather than a batch of frames, since we found this scheme yields faster convergence and slightly better fitting accuracy compared to training frame-by-frame. In this stage, NVF learns the temporal and motion priors of the given video, which facilitates subsequent consistent editing.

Field editing stage. We update the parameters of the trained NVF with a T2I model to impart editing effects, as shown in the right of Fig. 2. In each iteration, we input a coordinate set (X, Y, t) , where t means the frame number, X and Y are the sets of horizontal and vertical coordinates of pixels respectively. These three elements represent the coordinates of all pixels in a frame. NVF renders a frame based on them, as depicted in Fig. 2. Subsequently, the original frame is retrieved from the input video based on t as the image condition, whilst the user-provided instruction serves as the text condition. Consequently, we employ a T2I model to process the rendered frame and get an edited version $\bar{\mathbf{F}}_t$, which is used to optimize NVF. The objective function is:

$$\mathcal{L}_{\text{opt}}(\tilde{\theta}) = \|\tilde{f}_{\tilde{\theta}}(X, Y, t) - \bar{\mathbf{F}}_t\|_1. \quad (5)$$

Note that we only update NVF and fix the T2I model. Different from Sec. 3.2 that samples pixels randomly, here we supervise NVF frame-by-frame because T2I models exhibit optimal performance on complete images rather than irregularly sampled pixels. As only one frame is edited per iteration, our graphics memory requirement is constant and independent of the video length. Importantly, we adopt IP2P [3] as the T2I model, and further improve it for better editing effects, which is discussed in Sec. 3.3. It also proves that

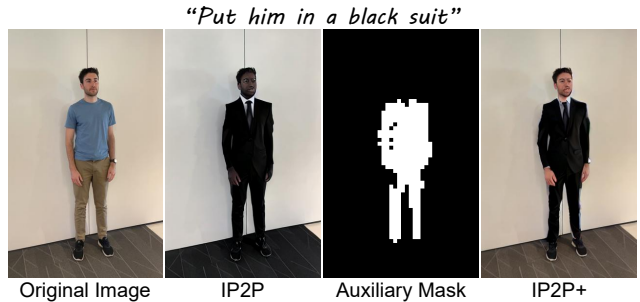


Figure 3. Visualization of the original image, the results of IP2P, the proposed auxiliary mask, and our edited results (IP2P+).

the T2I model of NVEdit is **replaceable** and **improvable**, related further experiments are given in Sec. 4.4.

In addition, a progressive optimization strategy is developed for temporal coherence. Specifically, At the beginning of the field editing stage, we assign a lower weight to the instruction condition, *i.e.*, setting s_P in Eq. 2 to a small number, and gradually increasing it as the optimization proceeds. This progressive strategy systematically guides the rendered frames toward the desired editing effects step-by-step, diminishing the updating intensity to NVF at each iteration. Thus, we effectively preserve the temporal priors of the NVF learned at the video fitting stage. Experiments validate the superior temporal consistency of our method.

Inference. After the completion of the aforementioned two stages, we render a coherent video $\tilde{\mathbf{V}}$ with the desired editing effects, using the trained NVF. We provide all pixel coordinates of the entire video, formulated as:

$$\tilde{\mathbf{V}} = \tilde{f}_{\tilde{\theta}}(X, Y, T), \quad (6)$$

where T is the set of all coordinates on the temporal axis.

3.3. Instruct-Pix2Pix+

Although IP2P enables impressive image editing effects, for local editing, it alters the region to be retained, as shown

in Fig. 3. We suppose this is an inherent flaw of IP2P, as it samples based on Eq. 2, which only ensures results to be roughly consistent with the image condition, but lacks strong constraints on the unedited region. Typically, users prefer instructing specific regions while leaving others untouched. To this end, we develop Instruct-Pix2Pix+ to enhance the content fidelity of edited images to the conditional image I , without any additional computation.

Auxiliary mask. The predicted noise of IP2P follows Eq. 2, where the third term indicates the guidance of instructions, as follows:

$$\varepsilon_{\theta_P} = \varepsilon_{\theta}(\mathbf{z}_t, \mathbf{c}_I, \mathbf{c}_P) - \varepsilon_{\theta}(\mathbf{z}_t, \mathbf{c}_I, \emptyset). \quad (7)$$

We observed that ε_{θ_P} represents the relationship between the generated image and conditional text. Hence, a simple yet effective auxiliary mask is proposed. We apply normalization and dimensionality reduction to ε_{θ_P} , getting a gray-scale image $\mathbf{G}_{x,I,T}$, in which a higher value x means the pixel is more likely to be relevant to instruction, and we allow it to change. In contrast, a lower x signals that the pixel is unlikely to require change. We set a mask threshold $\tau \in [0, 1]$ on $\mathbf{G}_{x,I,T}$ to get our auxiliary mask, $\mathbf{M}_{x,I,T} = \mathbb{1}(\mathbf{G}_{x,I,T} \geq \tau)$. Notice that we only use ε_{θ_P} , which is an essential element predicted in IP2P, to get $\mathbf{M}_{x,I,T}$, without any additional calculation.

Generation. According to [41], IP2P samples a latent \mathbf{z}_{t-1} at step $t-1$. With our auxiliary mask $\mathbf{M}_{x,I,T}$, the sampling latent of IP2P at timestep $t-1$ can be tuned as:

$$\mathbf{z}_{t-1} = \mathbf{z}_{t-1} \odot \mathbf{M}_{x,I,T} + \tilde{\mathbf{z}}_{t-1} \odot (\mathbf{1} - \mathbf{M}_{x,I,T}), \quad (8)$$

where \mathbf{z}_{t-1} is the latent generated by IP2P and $\tilde{\mathbf{z}}_{t-1}$ is the noisy latent of the conditional image I , which is also added the same level of noise as \mathbf{z}_{t-1} according to [41]. We thus only modify the latent of the most relevant region while preserving the original latent of other regions. Visual results are provided in Fig. 3 for a more intuitive illustration. Obviously, the vanilla IP2P inaccurately alters regions that should be preserved, such as the floor. With $\mathbf{M}_{x,I,T}$, IP2P+ edits the target objects and preserves original information well. Note that we only use auxiliary mask in the case of local editing. This enhanced version of IP2P also validates that the T2I model of NVEdit is adaptable.

4. Experiments

4.1. Implementation Details

To generate edited frames for optimizing NVE, we directly use the pre-trained IP2P [3] as the base model. The proposed auxiliary mask is introduced to improve its local editing capability. Following previous works [10, 17, 32], UVG-HD [23], DAVIS [31], and some other in-the-wild videos are adopted to evaluate the effect of our approach.

Metrics. Following [14, 32], we conduct quantitative evaluations using both objective (with the pre-trained CLIP [34] model) and subjective (with users) indicators. Specifically, three objective metrics are considered: **i) ‘Tem-Con’** measures the inter-frame temporal consistency. We only adopt the image encoder from CLIP, and compute the cosine similarity between all pairs of consecutive frames to obtain it. **ii) ‘Frame-Acc’** denotes the frame-wise editing accuracy, representing the percentage of frames from the edited video that have a higher CLIP similarity to the target prompt than the source prompt. **iii) ‘Vid-Score’** is the average value of the cosine similarity between edited frames and the target prompt, representing semantic disparity. Additionally, we enlist the evaluation of 21 volunteers to compute three subjective metrics, including **‘Edit’**, **‘Image’**, and **‘Temporal’**. These metrics gauge the coherency between edited frames and the target prompt, the quality of edited frames, and the temporal consistency of the edited video, respectively.

4.2. Comparison with the state-of-the-art

We prove our superior effectiveness by comparing with other five State-Of-The-Art (SOTA) text-driven video editing approaches, including Video-P2P [21], Vid2Vid-zero (V2V-zero) [43], TokenFlow [9], Fatezero [32], and CoDeF [29]. Furthermore, to demonstrate that the proposed method generates more temporal consistent results than directly applying the T2I model on videos, we fix the random seed of IP2P [3] and showcase its results as a baseline. All of these methods are recently proposed in 2023. Note that for prompt-to-prompt approaches, to ensure a fair comparison, we elaborate the source-target prompt pairs for them.

Quantitative comparison. We present both the objective and subjective metrics of our method and other recent SOTA algorithms. For subjective evaluation, we prepared 16 sets of edited results, shuffled the order of methods within each set, and asked users to rate different results in each set from 1 (the worst) to 5 (the best). As shown in Tab. 1, the proposed method achieves the best temporal consistency and frame-wise editing accuracy, and demonstrates comparable semantic alignment to the canonical image-based method [29] in the feature space of the CLIP model. As for user studies, on average, our approach obtains the best user preferences across three aspects.

Qualitative comparison. In order to provide a more intuitive comparison, we present the visual results of NVEdit and other baselines in two different scenarios in Fig. 4, showcasing two types of motion changes: the upper scenario changes action, while the lower one changes viewpoint. Instructions used in IP2P and our method are given above. For the prompt-to-prompt methods, we designed original prompts as ‘A man is walking his dog on the road in front of the courtyard’ and ‘A person stands before the wall’, whilst the target prompts are ‘A man is walking his

Metrics		IP2P	Video-P2P	V2V-zero	TokenFlow	Fatezero	CoDeF	Ours
CLIP \uparrow	Tem-Con	0.959	0.867	0.853	0.939	0.956	<u>0.972</u>	0.978
	Frame-Acc	<u>0.957</u>	0.893	0.800	0.852	0.838	0.955	0.961
	Vid-Score	0.342	0.297	0.282	0.274	0.266	0.348	<u>0.347</u>
User \uparrow	Edit	3.767	3.537	3.133	3.063	2.567	<u>3.833</u>	4.020
	Image	3.870	3.346	3.249	2.920	2.877	3.667	<u>3.755</u>
	Temporal	3.267	3.238	2.067	2.992	3.183	<u>3.967</u>	4.079

Table 1. Quantitative evaluation of the 16 sets of edited results obtained from different SOTA approaches proposed in 2023, including IP2P [3], Video-P2P [21], V2V-zero [43], TokenFlow [9], Fatezero [32], and CoDeF [29]. ‘Tem-Con’, ‘Frame-Acc’, and ‘Frame-Score’ are calculated by the pre-trained CLIP [34] model, while ‘Edit’, ‘Image’, and ‘Temporal’ are obtained from users. The best and the second-best scores are highlighted in **bold** and underline respectively.



Figure 4. Visual comparison between our method and other SOTA approaches. One can see that IP2P fails to output consistent results, such as the differences in the regions pointed by arrows. Other methods either distort the shape, mistake editing regions, or fail to respond to varying viewpoints. Our approach not only generates temporally coherent content but also controls the area to be edited precisely.

tiger on the road in front of the courtyard and *A person in pink shirt stands before the wall*. Observing the results, the edited results of frame-wise IP2P vary a lot among different frames (as indicated by the arrows) and fail to preserve unedited region (as shown in the bottom scene). Although other methods develop various techniques, such as attention-related control or null-text inversion, their results incorrectly modify the background and posture, or fail in certain viewpoints. Notice that CoDeF maps video content to a canonical image and edits it through ControlNet [50]. For a fair comparison, we use IP2P to edit the canon-

ical image of CoDeF in this paper, omitting the proposed auxiliary mask as it is a novel tool invented in this work. In the top-row example, the editing of the canonical image is occasionally subpar. However, CoDeF relies entirely on this edit, leading to an unsatisfactory appearance in all of its predicted frames. In contrast, our method, with progressive optimization using numerous pseudo-GTs, accommodates errors in certain pseudo-GTs. Besides, in the lower-row example, IP2P incorrectly colors the wall, consequently impacting the entire video of CoDeF, whereas our IP2P+ precisely controls the editable region to improve video editing.



Figure 5. NVEdit enables temporal consistent, high-quality edits of real-world long videos with hundreds of frames. The edited results not only faithfully conform to the instruction, but also strictly inherit original information, such as the posture, background, and motion.

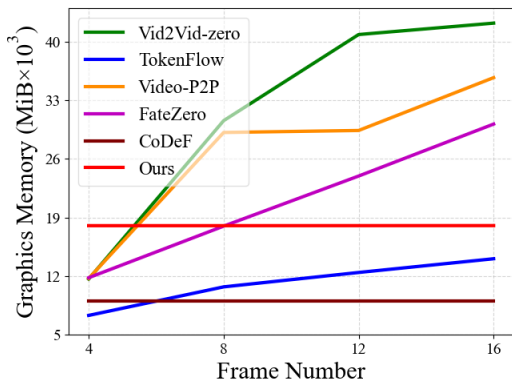


Figure 6. Comparison of graphics memory overhead. One can see that as frames increase, our method only adds minimal memory overhead, which allows it to edit long videos.

Graphics memory comparison. To demonstrate the superior graphics memory efficiency of our method, we record the graphics memory overhead of different algorithms using frames with a resolution of 480×480 . The experiments are conducted on a single NVIDIA A40 GPU. Due to its limited graphics memory, some methods cannot edit videos with more than 16 frames. Therefore, we selected 4, 8, 12, and 16 frames for our analysis. Results are displayed in a line chart to illustrate the memory growth trend of different methods. As depicted in Fig. 6, except CoDeF and our method, other approaches require inputting more frames to diffusion models for editing, resulting in a rapid increase in graphics memory. Although TokenFlow incurs a smaller cost than ours, its growth trend is evident, limiting its ability to edit long videos. Leveraging the efficient encoding of neural representation, both CoDeF and our method add only minor additional memory. Since CoDeF [29] employs an implicit representation, while we develop an explicit-implicit hybrid structure as discussed in Sec. 3.2, our graphics memory overhead is higher than that of CoDeF. How-



Figure 7. Results of frame interpolation. The water drop circled by yellow is changed from f_1 to f_2 while our method predicts this motion in $f_{1.5}$. Further, the editing effect is propagated continuously without any post-processing or fine-tuning.

ever, as noted in [6], our hybrid model enables a better representation effect than the implicit CoDeF. Besides, CoDeF maps video content to a canonical image, encoding only motion information, which reduces graphics memory demand. But for videos with significant variations, its mapping and encoding tend to be inaccurate. In contrast, our method encodes content and motion together through an effective hybrid structure, addressing this problem.

4.3. Application

Here we demonstrate some practical applications of NVEdit to establish that it not only enables multiple editing types (*e.g.*, changing shape, editing scene, and style transfer, *etc.*), but also accomplishes frame interpolation without any fine-tuning or post-processing operations.

Consistent video editing. Fig. 1 has displayed our results on various scenes and instructions, illustrating the temporal consistency and adherence to instructions achieved by our edits. On the left, we replace the wolf with other animals. The added animals maintain the same posture and motion as the wolf. Crucially, the background remains unchanged, whilst inter-frame variation is smooth and consistent throughout the edited video. On the right, we showcase the effects of scene and style editing. Our editing strictly follows the instructions, generating temporal consis-

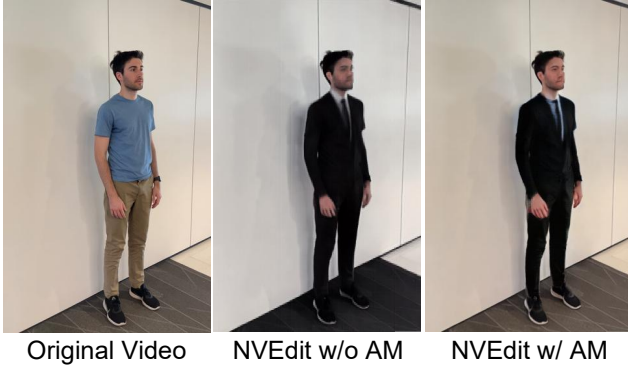


Figure 8. Results of NVEdit trained w/ and w/o our Auxiliary Mask (AM). Without AM, the background is incorrectly changed, while our final version achieves precise local editing.

tent videos while accurately inheriting original features. In addition, due to the impressive encoding efficiency, NVEdit enables long video editing. We present our results on long videos comprising 600 frames in Fig. 5, whose resolution is 960×544 . Again, different types of editing are applied to these videos. One can see that our method faithfully edits frames according to the user-given instructions, preserving information that does not require modification, such as motion and semantic layout, *etc.* Inter-frame consistency is also well-maintained after the field editing stage, allowing NVEdit to render editing effects without unnatural flickers.

Frame interpolation. Since the neural video field encodes a given video as a temporally continuous signal [17], we can seamlessly extend signals along the temporal axis, *i.e.*, frame interpolation, without any additional operations. Moreover, after the field editing stage, we can also effortlessly propagate the editing features to the predicted temporal signals. Illustrated in Fig. 7, NVEdit receives an instruction and edits frames in the original video (f_1 and f_2). We then adjust a hyper-parameter to extend its capability to render a longer video, *i.e.*, predicting novel frames that are not present in the original video ($f_{1.5}$). Notably, the new frame maintains coherence with its neighboring frames and the editing effect is seamlessly propagated to it.

4.4. Ablation Study

We mainly conduct an ablation study on the proposed Auxiliary Mask (AM), and substitute IP2P+ with an alternative image processing algorithm. The former demonstrates our improvement potential, while the latter validates the replacement ability for the T2I model within our framework.

Ablation on AM. As we have showcased AM and the results of IP2P and IP2P+ in Fig. 3, here we provide the rendered frames of the same instruction from NVEdit trained w/ and w/o the AM to underscore its importance. Since AM points out the editable regions for local editing, IP2P+ enables more precise editing and produces higher-quality pseudo-GTs to optimize our NVF. Therefore, as depicted



Figure 9. Video super-resolution results ($\times 4$) achieved by using an image super-resolution algorithm [44] to optimize the video field.

in Fig. 8, NVEdit outperforms the ablation setting, which exhibits a clearer face and an unchanged background.

Substitute the T2I model. Beyond IP2P, various image processing algorithms can be applied in NVEdit for diverse requirements. Here we take R-ESRGAN [44] as an example. By utilizing it to conduct image super-resolution on each rendered frame and produce pseudo-GT, our method seamlessly enhances the resolution of videos. Illustrated in Fig. 9, NVEdit initially fits a low-resolution video (top row), then optimized with pseudo-high-resolution ($\times 4$) GTs, achieving video super-resolution (bottom row).

5. Conclusion

This paper presents a memory-efficient framework NVEdit to edit videos with off-the-shelf image processing methods. We design a neural video field to enable long video editing and learn temporal priors for inter-frame consistency. In order to impart editing effects to the trained video field while preserving its temporal priors, a progressive optimization strategy is applied. Furthermore, to improve editing quality, we upgrade IP2P with the proposed auxiliary mask to benefit its precision in local editing, showcasing remarkable control over editable regions without additional computation, dubbed IP2P+. NVEdit outperforms existing baselines, demonstrating substantial improvements in local editing, temporal consistency, and the length of editable video. At last, we shed the unique advantages and immense potential of neural representations in video editing, illustrating how they can be synergized with T2I models. Both the video field and IP2P+ can be replaced or improved for various requirements, which inspires future research.

Limitations. Although we have achieved SOTA consistency in editing, temporal priors are still inevitably affected to some extent in the field editing stage. Moreover, the increased frames require more iterations in the field editing stage, resulting in more time costs. We suppose that, in the future, only editing keyframes and using frame interpolation of NVF to propagate the editing effect throughout the entire video is a potential acceleration solution.

Neural Video Fields Editing

Supplementary Material

Algorithm 1 NVEdit Algorithm

Require:

- $\tilde{\theta}$: Parameters of the desired video field $f(\tilde{\theta})$
- *Edit*: The chosen T2I model

Input:

- \mathbf{V} : Source video
- P : User-given instruction

▷ **The video fitting stage**

while not converge **do**

$$\tilde{\mathbf{V}}[x, y, t] = f_{\tilde{\theta}}(x, y, t)$$

$$\tilde{\theta} \leftarrow \operatorname{argmin}_{\tilde{\theta}} \sum_{(x, y, t) \in \psi} \|\mathbf{V}[x, y, t] - \tilde{\mathbf{V}}[x, y, t]\|_2^2 \triangleright \mathcal{L}_{\text{fit}}(\tilde{\theta})$$

end while

▷ **The field editing stage**

while not converge **do**

$$\tilde{\mathbf{F}}_t = f_{\tilde{\theta}}(\mathbf{X}, \mathbf{Y}, t)$$

$$\tilde{\mathbf{F}}_t = \text{Edit}(\tilde{\mathbf{F}}_t, \mathbf{V}[\mathbf{X}, \mathbf{Y}, t], P) \quad \triangleright \text{Edit the frame}$$

$$\tilde{\theta} \leftarrow \operatorname{argmin}_{\tilde{\theta}} \|\tilde{\mathbf{F}}_t - \tilde{\mathbf{F}}_t\|_1 \quad \triangleright \mathcal{L}_{\text{opt}}(\tilde{\theta})$$

end while

▷ **Inference**

function INFERENCE($\mathbf{X}, \mathbf{Y}, T$)

$$\tilde{\mathbf{V}} = f_{\tilde{\theta}}(\mathbf{X}, \mathbf{Y}, T) \quad \triangleright \text{Eq. 6 in main paper}$$

return $\tilde{\mathbf{V}}$

end function

Output:

- $\tilde{\mathbf{V}}$: Final edited video
-

6. Implementation Details

Pseudo algorithm code. Our full algorithm is shown in Algorithm 1, which includes the process of video fitting, field editing, and inference. NVEdit first learns motion and temporal priors of the given video (video fitting stage). Then a T2I model is applied to edit the rendered frame $\tilde{\mathbf{F}}_t$, which is utilized to update the neural video field for editing effects (field editing stage). Here we adopt Instruct-Pix2Pix+ as the function *Edit*. Finally, the edited video can be rendered through the trained parameters.

Hyperparameters. We mainly introduce three hyperparameters in the proposed method:

- $t_u \in [1, T]$: The upper boundary for the initial sampling timestep in Instruct-Pix2Pix+. A smaller value results in a diminished editing amplitude, whereas a larger value corre-



Figure 10. Visual results of the composed editing. We recurrently run the field editing stage with different instructions to achieve blended editing effects.

sponds to a more pronounced editing effect.

- $t_l \in [1, T]$: The lower limit for the initial sampling timestep in Instruct-Pix2Pix+. Bigger t_l correlates with a greater edit.

- (Optional) $\tau \in [0, 1]$: The threshold for our auxiliary mask used in Instruct-Pix2Pix+, which is only adopted in the case of local editing. Bigger τ enables larger editable region.

In the context of **global** editing, we set $t_u = 0.98T$ and $t_l = 0.42T$, with the omission of an auxiliary mask. For **local** editing, we set $t_u = 0.98T$ and $t_l = 0.82T$. $\tau = 0.1$ is an empirical value, which has been able to perform well in most applications and users can adjust it slightly based on their specific requirements.

7. More Visual Results

You can further view more editing results in our [project](#). In this section, we succinctly introduce an extension work (composed editing) and furnish additional subjective results to substantiate the efficacy of NVEdit. All results provided in this section are available in our [project](#).

Composed editing. In the main paper, we have implemented text-driven editing based on the user-given instructions. Furthermore, we attempt to apply field editing stage recurrently with different instructions to achieve composed editing. As depicted in Fig. 10, the image in the third column simultaneously satisfies both instructions, validating the feasibility of composed editing achieved through the recurrent invocation of the field editing stage.

More editing results. NVEdit enables multiple types of editing, including style transfer and shape variation. To further validate its superior editing capabilities, in Fig. 11, we provide additional four sets of editing results. Each set comprises the original video displayed in the upper line, juxtaposed with the corresponding edited results in the lower line. We provide their related editing instructions under the edited videos of each set.

Long video editing. Notice that NVEdit enables high-quality editing for long videos, exhibiting a significant practical merit. For a more intuitive validation, detailed results are elucidated in Fig. 12, which includes a 50-frame original video juxtaposed with its edited version. We turn the



Figure 11. Four sets of visual results from NVEdit, which enables multiple types of editing, including style transfer and shape variation. The instructions for editing are noted under each set.



Figure 12. Editing results of a long video. The frame number is provided below each image (from f_1 to f_{50} .)

running horse into a donkey and the corresponding frame numbers (from f_1 to f_{50}) are annotated beneath their respective outcomes. More long video editing results can be accessed in our [project](#).

8. Comparison on Runtime

Due to the optimization strategy in the field editing stage, our training time scales linearly with the duration of the

videos to be edited, as discussed in the limitation part of the main paper. We provide a detailed quantitative comparison in Tab. 2, which compares the runtime of different methods on videos with different frame numbers, including 4, 8, 12, and 16. Their resolution is all 480×480 . One can see that our time cost is slightly higher than that of the compared SOTA methods. It is important to note, however, that these SOTA methods face constraints in editing lengthy videos due to finite GPU memory, whereas NVEdit successfully

Method	Runtime (s)			
	4	8	12	16
TokenFlow	126.51	211.8	283.24	404.19
Video-P2P	212.82	367.06	512.38	677.37
V2V-zero	116.05	235.05	371.26	518.29
Fatezero	76.67	129.41	175.19	224.77
CoDeF	256.34	397.61	649.62	997.99
Ours	428.79	609.72	905.97	1104.26

Table 2. The comparison of different methods in terms of runtime costs. Experiments are conducted on a single NVIDIA A40 GPU, using videos at a resolution of 480×480 .

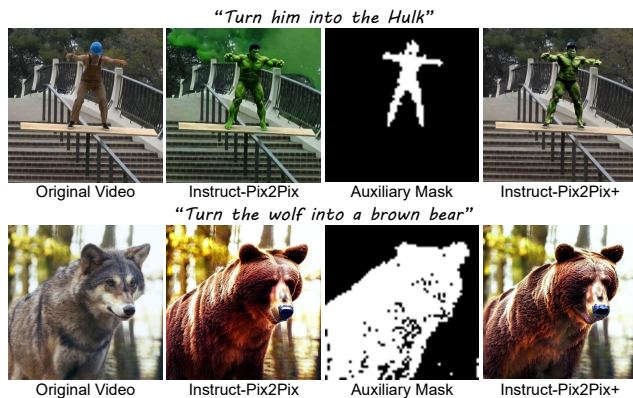


Figure 13. Some visual samples of the original image, the results of IP2P, the proposed auxiliary mask, and results of IP2P+.

overcomes this limitation, as illustrated in Fig. 12. To accelerate editing, we suppose that instead of sampling frames across the entire video, assign key frames in advance and only edit them for supervision in the field editing stage is a feasible solution.

9. Limitation and Future Work

We impart editing effects through the field editing stage, which makes our performance to be constrained by the effectiveness of the chosen T2I model. To enhance the editing effects, we applied IP2P+ in the main paper. Notice that NVEdit also supports other image editing or processing algorithms, which enables different editing effects and even various downstream video tasks, *e.g.*, the adoption of R-ESRGAN in Sec. 4.4 of the main paper for video super-resolution. We leave further research to future work.

10. Results of Instruct-Pix2Pix+

In this paper, we develop a competitive text-driven image editing algorithm, called Instruct-Pix2Pix+ (IP2P+), which achieves impressive effects in local editing without any additional computation. Details have been discussed in Sec. 3.3 of the main paper. Here we additionally provide some results of this valuable image editing approach in Fig. 13. Hoping that this innovation inspires future arti-

cial intelligence generative content work.

References

- [1] Improving image generation with better captions. <https://cdn.openai.com/papers/dall-e-3.pdf>, 2023. 2
- [2] Yunpeng Bai, Chao Dong, and Cairong Wang. Ps-nerv: Patch-wise stylized neural representations for videos. In *arXiv*, 2022. 2, 3
- [3] Tim Brooks, Aleksander Holynski, and Alexei A. Efros. Instructpix2pix: Learning to follow image editing instructions. In *Proceedings of the IEEE/CVF Conference on Computer Vision and Pattern Recognition*, 2023. 2, 3, 4, 5, 6
- [4] Duygu Ceylan, Chun-Hao P. Huang, and Niloy J. Mitra. Pix2video: Video editing using image diffusion. In *Proceedings of the IEEE/CVF International Conference on Computer Vision*, 2023. 1
- [5] Wenhao Chai, Xun Guo, Gaoang Wang, and Yan Lu. Stable-video: Text-driven consistency-aware diffusion video editing. In *Proceedings of the IEEE/CVF International Conference on Computer Vision*, 2023. 1
- [6] Eric R. Chan, Connor Z. Lin, Matthew A. Chan, Koki Nagano, Boxiao Pan, Shalini De Mello, Orazio Gallo, Leonidas J. Guibas, Jonathan Tremblay, Sameh Khamis, Tero Karras, and Gordon Wetzstein. Efficient geometry-aware 3d generative adversarial networks. In *Proceedings of the IEEE/CVF Conference on Computer Vision and Pattern Recognition (CVPR)*, 2022. 7
- [7] Hao Chen, Bo He, Hanyu Wang, Yixuan Ren, Ser Nam Lim, and Abhinav Shrivastava. Nerv: Neural representations for videos. In *Advances in Neural Information Processing Systems*, 2021. 2, 3
- [8] Patrick Esser, Johnathan Chiu, Parmida Atighehchian, Jonathan Granskog, and Anastasis Germanidis. Structure and content-guided video synthesis with diffusion models. In *Proceedings of the IEEE/CVF International Conference on Computer Vision*, 2023. 1
- [9] Michal Geyer, Omer Bar-Tal, Shai Bagon, and Tali Dekel. Tokenflow: Consistent diffusion features for consistent video editing. In *arXiv*, 2023. 2, 5, 6
- [10] Ayaan Haque, Matthew Tancik, Alexei A. Efros, Aleksander Holynski, and Angjoo Kanazawa. Instruct-nerf2nerf: Editing 3d scenes with instructions. In *arXiv*, 2023. 2, 5
- [11] Amir Hertz, Ron Mokady, Jay Tenenbaum, Kfir Aberman, Yael Pritch, and Daniel Cohen-or. Prompt-to-prompt image editing with cross-attention control. In *The Eleventh International Conference on Learning Representations*, 2023. 1
- [12] Jonathan Ho, Ajay Jain, and Pieter Abbeel. Denoising diffusion probabilistic models. In *Advances in Neural Information Processing Systems*, 2020. 3
- [13] Jonathan Ho, Tim Salimans, Alexey Gritsenko, William Chan, Mohammad Norouzi, and David J Fleet. Video diffusion models. In *arXiv*, 2022. 2
- [14] Nisha Huang, Yuxin Zhang, and Weiming Dong. Style-a-video: Agile diffusion for arbitrary text-based video style transfer. In *arXiv*, 2023. 5

- [15] Yoni Kasten, Dolev Ofri, Oliver Wang, and Tali Dekel. Layered neural atlases for consistent video editing. *ACM Trans. Graph.*, 2021. [2](#), [3](#)
- [16] Levon Khachatryan, Andranik Movsisyan, Vahram Tadevosyan, Roberto Henschel, Zhangyang Wang, Shant Navasardyan, and Humphrey Shi. Text2video-zero: Text-to-image diffusion models are zero-shot video generators. In *arXiv*, 2023. [2](#)
- [17] Subin Kim, Sihyun Yu, Jaeho Lee, and Jinwoo Shin. Scalable neural video representations with learnable positional features. In *Advances in Neural Information Processing Systems*, 2022. [2](#), [3](#), [5](#), [8](#)
- [18] Nupur Kumari, Bingliang Zhang, Richard Zhang, Eli Shechtman, and Jun-Yan Zhu. Multi-concept customization of text-to-image diffusion. In *Proceedings of the IEEE/CVF Conference on Computer Vision and Pattern Recognition*, 2023. [2](#)
- [19] Zizhang Li, Mengmeng Wang, Huaijin Pi, Kechun Xu, Jianbiao Mei, and Yong Liu. E-nerv: Expedite neural video representation with disentangled spatial-temporal context. In *arXiv*, 2022. [2](#), [3](#)
- [20] Jun Hao Liew, Hanshu Yan, Jianfeng Zhang, Zhongcong Xu, and Jiashi Feng. Magicedit: High-fidelity and temporally coherent video editing. In *arXiv*, 2023. [2](#)
- [21] Shaoteng Liu, Yuechen Zhang, Wenbo Li, Zhe Lin, and Jiaya Jia. Video-p2p: Video editing with cross-attention control. In *arXiv*, 2023. [5](#), [6](#)
- [22] Chenlin Meng, Yutong He, Yang Song, Jiaming Song, Jiajun Wu, Jun-Yan Zhu, and Stefano Ermon. SDEdit: Guided image synthesis and editing with stochastic differential equations. In *International Conference on Learning Representations*, 2022. [1](#)
- [23] Alexandre Mercat, Marko Viitanen, and Jarno Vanne. Uvg dataset: 50/120fps 4k sequences for video codec analysis and development. In *Proceedings of the 11th ACM Multimedia Systems Conference*, 2020. [5](#)
- [24] Ben Mildenhall, Pratul P. Srinivasan, Matthew Tancik, Jonathan T. Barron, Ravi Ramamoorthi, and Ren Ng. Nerf: Representing scenes as neural radiance fields for view synthesis. *Commun. ACM*, 2021. [2](#)
- [25] Ron Mokady, Amir Hertz, Kfir Aberman, Yael Pritch, and Daniel Cohen-Or. Null-text inversion for editing real images using guided diffusion models. In *Proceedings of the IEEE/CVF Conference on Computer Vision and Pattern Recognition*, 2023. [1](#)
- [26] Eyal Molad, Eliahu Horwitz, Dani Valevski, Alex Rav Acha, Yossi Matias, Yael Pritch, Yaniv Leviathan, and Yedid Hoshen. Dreamix: Video diffusion models are general video editors. In *arXiv*, 2023. [1](#)
- [27] Chong Mou, Xintao Wang, Liangbin Xie, Yanze Wu, Jian Zhang, Zhongang Qi, Ying Shan, and Xiaohu Qie. T2i-adapt: Learning adapters to dig out more controllable ability for text-to-image diffusion models. In *arXiv*, 2023. [1](#)
- [28] Alexander Quinn Nichol, Prafulla Dhariwal, Aditya Ramesh, Pranav Shyam, Pamela Mishkin, Bob McGrew, Ilya Sutskever, and Mark Chen. GLIDE: Towards photorealistic image generation and editing with text-guided diffusion models. In *Proceedings of the 39th International Conference on Machine Learning*, 2022. [2](#)
- [29] Hao Ouyang, Qiuyu Wang, Yuxi Xiao, Qingyan Bai, Juntao Zhang, Kecheng Zheng, Xiaowei Zhou, Qifeng Chen, and Yujun Shen. Codef: Content deformation fields for temporally consistent video processing. In *arXiv*, 2023. [2](#), [3](#), [5](#), [6](#), [7](#)
- [30] Dustin Podell, Zion English, Kyle Lacey, Andreas Blattmann, Tim Dockhorn, Jonas Müller, Joe Penna, and Robin Rombach. Sdxl: Improving latent diffusion models for high-resolution image synthesis. In *arXiv*, 2023. [2](#)
- [31] Jordi Pont-Tuset, Federico Perazzi, Sergi Caelles, Pablo Arbeláez, Alex Sorkine-Hornung, and Luc Van Gool. The 2017 davis challenge on video object segmentation. In *arXiv*, 2018. [5](#)
- [32] Chenyang Qi, Xiaodong Cun, Yong Zhang, Chenyang Lei, Xintao Wang, Ying Shan, and Qifeng Chen. Fatezero: Fusing attentions for zero-shot text-based video editing. In *arXiv*, 2023. [2](#), [5](#), [6](#)
- [33] Bosheng Qin, Juncheng Li, Siliang Tang, Tat-Seng Chua, and Yueting Zhuang. Instructvid2vid: Controllable video editing with natural language instructions. In *arXiv*, 2023. [1](#), [2](#)
- [34] Alec Radford, Jong Wook Kim, Chris Hallacy, Aditya Ramesh, Gabriel Goh, Sandhini Agarwal, Girish Sastry, Amanda Askell, Pamela Mishkin, Jack Clark, Gretchen Krueger, and Ilya Sutskever. Learning transferable visual models from natural language supervision. In *Proceedings of the 38th International Conference on Machine Learning*, 2021. [5](#), [6](#)
- [35] Robin Rombach, Andreas Blattmann, Dominik Lorenz, Patrick Esser, and Björn Ommer. High-resolution image synthesis with latent diffusion models. In *Proceedings of the IEEE/CVF Conference on Computer Vision and Pattern Recognition*, 2022. [2](#), [3](#)
- [36] Nataniel Ruiz, Yuanzhen Li, Varun Jampani, Yael Pritch, Michael Rubinstein, and Kfir Aberman. Dreambooth: Fine tuning text-to-image diffusion models for subject-driven generation. In *Proceedings of the IEEE/CVF Conference on Computer Vision and Pattern Recognition*, 2023. [2](#)
- [37] Chitwan Saharia, William Chan, Saurabh Saxena, Lala Li, Jay Whang, Emily L Denton, Kamyar Ghasemipour, Raphael Gontijo Lopes, Burcu Karagol Ayan, Tim Salimans, Jonathan Ho, David J Fleet, and Mohammad Norouzi. Photorealistic text-to-image diffusion models with deep language understanding. In *Advances in Neural Information Processing Systems*, 2022. [2](#)
- [38] Chaehun Shin, Heeseung Kim, Che Hyun Lee, Sang gil Lee, and Sungroh Yoon. Edit-a-video: Single video editing with object-aware consistency. In *arXiv*, 2023. [1](#)
- [39] Uriel Singer, Adam Polyak, Thomas Hayes, Xi Yin, Jie An, Songyang Zhang, Qiyuan Hu, Harry Yang, Oron Ashual, Oran Gafni, Devi Parikh, Sonal Gupta, and Yaniv Taigman. Make-a-video: Text-to-video generation without text-video data. In *The Eleventh International Conference on Learning Representations*, 2023. [1](#), [2](#)
- [40] Vincent Sitzmann, Julien Martel, Alexander Bergman, David Lindell, and Gordon Wetzstein. Implicit neural representa-

- tions with periodic activation functions. In *Advances in Neural Information Processing Systems*, 2020. 3
- [41] Jiaming Song, Chenlin Meng, and Stefano Ermon. Denoising diffusion implicit models. In *International Conference on Learning Representations*, 2021. 1, 5
- [42] Narek Tumanyan, Michal Geyer, Shai Bagon, and Tali Dekel. Plug-and-play diffusion features for text-driven image-to-image translation. In *Proceedings of the IEEE/CVF Conference on Computer Vision and Pattern Recognition*, 2023. 2
- [43] Wen Wang, Kangyang Xie, Zide Liu, Hao Chen, Yue Cao, Xinlong Wang, and Chunhua Shen. Zero-shot video editing using off-the-shelf image diffusion models. In *arXiv*, 2023. 2, 5, 6
- [44] Xintao Wang, Liangbin Xie, Chao Dong, and Ying Shan. Real-esrgan: Training real-world blind super-resolution with pure synthetic data. In *Proceedings of the IEEE/CVF International Conference on Computer Vision Workshops*, 2021. 8
- [45] Yinhuai Wang, Shuzhou Yang, Yujie Hu, and Jian Zhang. Nerfocus: Neural radiance field for 3d synthetic defocus. In *arXiv*, 2022. 2
- [46] Yuanzhi Wang, Yong Li, Xin Liu, Anbo Dai, Antoni Chan, and Zhen Cui. Edit temporal-consistent videos with image diffusion model. In *arXiv*, 2023. 1
- [47] Jay Zhangjie Wu, Yixiao Ge, Xintao Wang, Stan Weixian Lei, Yuchao Gu, Yufei Shi, Wynne Hsu, Ying Shan, Xiaohu Qie, and Mike Zheng Shou. Tune-a-video: One-shot tuning of image diffusion models for text-to-video generation. In *Proceedings of the IEEE/CVF International Conference on Computer Vision*, 2023. 1, 2
- [48] Shuzhou Yang, Moxuan Ding, Yanmin Wu, Zihan Li, and Jian Zhang. Implicit neural representation for cooperative low-light image enhancement. In *Proceedings of the IEEE/CVF International Conference on Computer Vision*, 2023. 3
- [49] Shuai Yang, Yifan Zhou, Ziwei Liu, and Chen Change Loy. Rerender a video: Zero-shot text-guided video-to-video translation. In *arXiv*, 2023. 1
- [50] Lvmin Zhang, Anyi Rao, and Maneesh Agrawala. Adding conditional control to text-to-image diffusion models. In *Proceedings of the IEEE/CVF International Conference on Computer Vision*, 2023. 6
- [51] Yunfan Zhang, Ties van Rozendaal, Johann Brehmer, Markus Nagel, and Taco Cohen. Implicit neural video compression, 2021. 3
- [52] Zhixing Zhang, Ligong Han, Arnab Ghosh, Dimitris N. Metaxas, and Jian Ren. Sine: Single image editing with text-to-image diffusion models. In *Proceedings of the IEEE/CVF Conference on Computer Vision and Pattern Recognition*, 2023. 2